Structural and electronic properties of the *in situ* impurity As_{Hg} in $Hg_{0.5}Cd_{0.5}Te$: First-principles study

L. Z. Sun, X. S. Chen,* Y. L. Sun, X. H. Zhou, Zh. J. Quan, He Duan, and Wei Lu
National Laboratory for Infrared Physics, Shanghai Institute of Technical Physics, Chinese Academy of Science, 200083 Shanghai, China
(Received 28 September 2004; revised manuscript received 30 November 2004; published 25 May 2005)

The structural and electronic properties of the *in situ* impurity As_{Hg} in $Hg_{0.5}Cd_{0.5}Te$ (MCT) have been studied by using the density-functional theory within the full-potential linear augmented plane wave method. The supercell with 64 atoms has been considered in the calculations. The relaxation, local charge density, and density of states are shown to discuss the effects of local environment induced by impurity on the electronic structure. The *in situ* As_{Hg} impurity in $Hg_{0.5}Cd_{0.5}Te$ exhibits a single donor level to be close to the conduction-band minimum (CBM), and the donor level position is quantitatively determined to be 9 meV below the CBM, in agreement with the experimental results of the photoluminescence.

DOI: 10.1103/PhysRevB.71.193203 PACS number(s): 71.55.Gs, 71.20.Nr, 71.15.Pd

Mercury cadmium telluride ($Hg_{1-x}Cd_xTe$) is currently one of the most widely used semiconductor materials for infrared detector arrays. It is well known that the applications of the semiconductor materials especially for II-VI compounds and alloys mainly depend on whether they can be doped with a donor or acceptor.[1] For infrared detectors fabricated by $Hg_{1-x}Cd_xTe$ (MCT), the *p* on *n* heterojunction is currently the preferred device design. In recent years, due to its low diffusivity in $Hg_{1-x}Cd_xTe$ [2] compared with the native acceptor and the group I elements, attentions have focused on the group V elements, especially arsenic, as the *p*-type dopant. The experimental results have indicated that arsenic can provide a shallow acceptor level in molecular-beam epitaxy (MBE) HgCdTe.[3] But the arsenic doping is strongly self-compensated, requiring annealing for its *p*-type electric activation.[4] At the same time, the amphoteric behavior of arsenic in HgCdTe has been found in materials grown by bulk method,[5] liquid phase epitaxy (LPE),[6] and MBE,[7] with incorporation as a *p*-type dopant under Hg-rich conditions, and as an *n*-type dopant or inactive dopant under Te-rich conditions. Although MBE is done at much lower temperatures than LPE, and thus offers some distinct advantages, the group V impurities are still observed to incorporate as donors,[8] self-compensating the *p*-type doping. Reference 9 has shown that there is a significant fraction of the arsenic residing on the cation sublattice even under cation-saturated conditions. According to the arsenic dopant incorporation model[10] and the quasichemical predictions,[11,12] some of the doped arsenics in MCT grown by MBE are incorporated on the cation sublattice as isolated defects, As_{Hg}, unbound to vacancies, as donors. Although the arsenic incorporation can be switched from *n*- to *p*-type through post-growth annealing, the electronic properties of *in situ* As_{Hg} not only determine the material properties before annealing, but also mainly dominate the annealing activation process from *n*- to *p*-type. Moreover, for doping levels above 5×10^{18} cm^{-3}, the As activation efficiency drastically drops because of the As_{Hg} self-compensation[13,14]. Although the models of the amphoteric behavior have been suggested, there is not a comprehensive consensus on the microscopic mechanism of group V impurity incorporation in MCT, which is essentially important for infrared focal plane array technology. There are some theoretical studies of arsenic-doped MCT materials. However, the calculations reported with the *ab initio* method, to our knowledge, are lacking. Therefore, we have carried out full-potential linear augmented plane wave (FP-LAPW) total energy calculations to investigate the effect of As_{Hg} impurities on the electronic properties, the structural relaxation, and the bonding mechanism in $Hg_{0.5}Cd_{0.5}Te$. The reason for the mole fraction chosen in the present paper is that the calculation results can be compared with the thoroughly studied II-VI semiconductors (CdTe and HgTe) to some extent. On the other hand, the results can be easily extrapolated to the other mole fraction compositions. It is well known that MCT is a pseudobinary alloys, which means the two type cations occupy randomly the cation sites. The disorder may have some effect on the electronic properties of the doped MCT. In order to simplify the calculation procedure, we only chose the perfect quasi-zinc-blende crystal structure as the basis of the supercell (SC), and the disorder effect is neglected in the present paper because it is very time-consuming work.

Within the framework of the density-functional theory[15] in combination with the Perdew-Burke-Ernzerhof (PBE) exchange-correlation potential,[16] our calculations are performed by using the WIEN2K package,[17] the implementation of the FP-LAPW method. We have considered a $2\times2\times2$ SC of 64 atoms consisting of eight $Hg_{0.5}Cd_{0.5}Te$ unit cells in quasi-zinc-blende crystal structure. One of 16 mercury atoms in the SC is replaced by an arsenic atom as dopant. The $2\times2\times1$ SC of 32 atoms without As impurity has been chosen as a comparable reference. The satisfactory convergence has been achieved by considering the FP-LAPW basis functions up to $R_{MT}K_{max}=6.0$ for the SC, where R_{MT} is the muffin-tin (MT) radius and K_{max} is the maximum value of the plane-wave vector which determines the so-called energy cutoff for the plane-wave expansion. The states treated as valence are Hg ($5d^{10}6s^2$), Cd ($4d^{10}5s^2$), Te ($5s^25p^4$), and As ($3d^{10}4s^24p^3$), respectively. The muffin-tin radii are 2.60 atomic units (a.u.) for all four kinds of atoms. Eight and 32 *k* points in the irreducible Brillouin zone have been chosen for

 ©2005 The American Physical Society

TABLE I. The relaxation of NN (Te) and NNN (Cd,Hg) around the arsenic and the bond length change between NN (Te) and NNN (Cd,Hg) atoms. The positive and negative signs mean outward relaxation and inward relaxation, respectively. The unit of the bond length and the distance change is Å. The superscript is the number of the atomic shells around As.

	As-Te^1	As-Cd^2	As-Hg^2	Te^1-Hg^2	Te^1-Cd^2
Prelaxation	2.831	4.624	4.624	2.831	2.831
After relaxation	2.826	4.638	4.649	2.856	2.863
Change	–0.010	0.013	0.021	0.025	0.028
Change ratio	–0.37%	0.28%	0.47%	0.89%	0.99%

doped and pure $Hg_{0.5}Cd_{0.5}Te$, respectively. The localized levels are deduced from the calculations of the single electron energy levels at the Γ point and are aligned using core electron energy levels. The relaxation procedures are calculated following the damped Newton dynamic schemes.[18–20] The relativistic effect of spin-orbit (SO) coupling is also included.

It is well known that impurities induce the atomic structural relaxation in the host and modify the electronic structure of the system. Before the relaxation calculations, the equilibrium volumes have been obtained for doped and undoped materials from the calculated total energy versus different volumes around the lattice constants given by Vegard's law. All the calculated values are fitted to the Murnaghan equation of state.[21] In comparison with the experimental results, the optimized bond lengths of R(Te-Cd) and R(Te-Hg) are about 1% larger than that of experiments for CdTe and HgTe. Due to the little mismatch of the lattice constants of CdTe and HgTe in the alloys of MCT (smaller than 0.3%), the calculated bond length relaxations of MCT are less than 0.1% in the present work. In Table I, the relaxation results of arsenic-doped $Hg_{0.5}Cd_{0.5}Te$ are listed. From the relaxation results, we can find that the NN tellurium atoms show 0.37% inward relaxation. In contrast, the NNN cations show outward relaxation, 0.28% for Cd and 0.47% for Hg relative to the impurity. Further, the relaxation of the bond angles around the impurity indicates that the inhomogenous cation configuration around the NN tellurium makes it relax along the arrow as shown in Fig. 1, which produces an inverse change of the bond angles α and $\beta(\alpha > \beta)$. The bond angle relaxation causes the bond length of Te^1-Hg^2 smaller than that of Te^1-Cd^2.

In order to understand the bonding mechanism of arsenic doping on $Hg_{0.5}Cd_{0.5}Te$, the valence charge density and the bonding-charge density[22] have been calculated. The bonding charge density is defined as the difference between the total charge density in the solid and the superpositions of neutral atomic charge densities located at atomic sites, i.e.,

$$\Delta\rho(r) = \rho_{solid}(r) - \sum_{\alpha} \rho_{\alpha}(r - r_{\alpha}). \qquad (1)$$

Therefore, the bonding-charge density represents the net charge redistribution as atoms are brought together to form the crystal. Figure 2 shows the valence charge density and the bonding-charge density on the (110) plane. From the figure, we can see that the charge-density distribution between the arsenic impurity and NN tellurium atoms shows the covalent characteristic. The valence charge density along the As-Te bond line has been picked up as shown in Fig. 3, which indicates that it is a nearly perfect covalent bond. Besides, the smaller radius of arsenic than that of mercury causes the NN tellurium to relax inwardly; the stronger covalent bonding also results in NN Te inward relaxation.

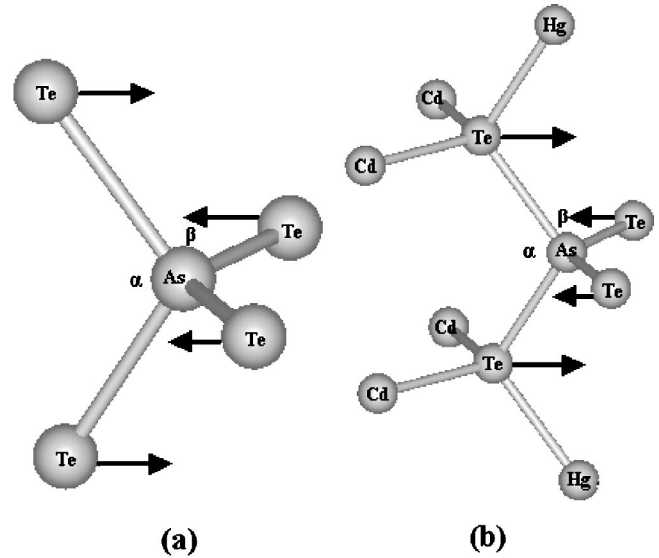

FIG. 1. The diagram of the relaxation process of the NN tellurium atoms around the arsenic.

In the LAPW formalisms, a unit cell is partitioned into two types of regions, namely the sphere around the atoms (MT sphere) and the interstitial region. Due to this spatial decomposition, the charge distribution is also partitioned into two corresponding regions. It is instructive to compare the total valence charge of the doped materials with that of the undoped one for the corresponding site ions with the same size MT spheres (which is the basis for the comparison in a different compound[23]). The charge-transfer results, listed in

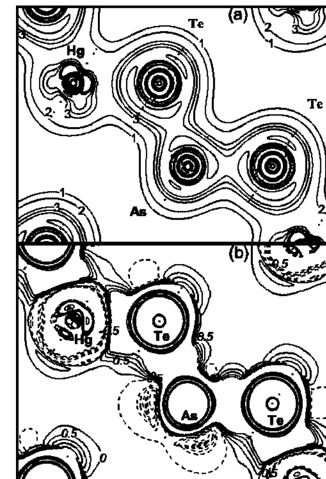

FIG. 2. The total charge density in the (110) plane, where the contour step size is 6×10^{-3} $e/(\mathrm{a.u.})^3$.

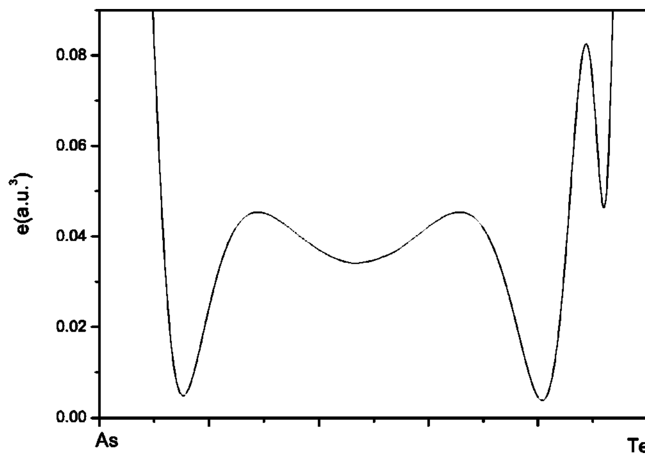

FIG. 3. The total charge density along the bond line of As-Te.

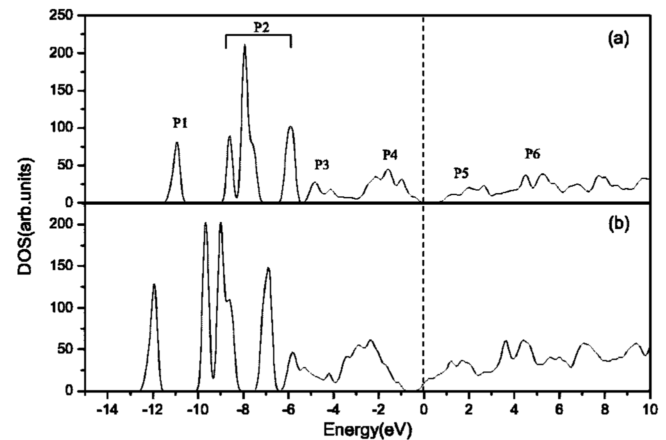

FIG. 4. The total DOS of undoped MCT (a) and As_{Hg} MCT (b); Fermi level is set to zero. The following Fermi level in the DOS figures is in the same way.

Table II, indicate that the impurity influences not only the charge redistribution of the nearest neighbors, but also that of the NNN cations.

The total and partial DOS are calculated by using the modified tetrahedron integration method[24] and are broadened by using a Gaussian-like function with full width at half maximum (FWHM) being equal to 0.1 eV. The DOS of undoped and doped $Hg_{0.5}Cd_{0.5}Te$ are shown in Figs. 4(a) and 4(b), respectively. In comparison with the undoped materials, the valence bandwidth of the As-doped materials is broadened about 176 meV due to the two extra As $4p$ bonding states coupling into the valence band. Substitution of mercury by arsenic makes the As-doped MCT metallic because an electron of the As-p state fills up to the conduction band. The Fermi level does not lie within the band gap, but it extends to the conduction band, as shown in Fig. 4(b). Following the principle discussed in Ref. 25, for simple extrinsic impurities, one in principle can predict whether a dopant is a donor or an acceptor by simply counting the number of the valence electrons of the dopant and the host elements. Here, the integral of the density of states from CBM to the Fermi level accommodates one electron occupying the t_2^c state. The energy state behaves as a single donor. The results agree with the theoretical[11,12] and experimental[5,6,10] findings, where the impurity As_{Hg} in $Hg_{0.5}Cd_{0.5}Te$ behaves as a single donor. Because the Gaussian broadened factor is different from Ref. 26, our results show some fine structures on the band edge. By comparing Fig. 4(a) with Fig. 4(b), we can find that the band edge of As-doped MCT shows more apparent shoulders than that of the perfect MCT. The difference mainly comes from the coupling of As-s and NN Te-p at the VBM, and the coupling of As-p and the NNN cation-s at the CBM. So, we can predict that the single donor of As_{Hg}-doped $Hg_{0.5}Cd_{0.5}Te$ mainly comes from the coupling of the As-p and the NNN cation-s states. The coupling strength is determined by the distance between the impurity and the native atoms in the host. Figure 5 shows that the effect of the coupling strength between the impurity and host atoms on the conduction-band edge is reduced as the distance become larger. The results of the calculated band gaps (0.476 eV and 0.457 eV for undoped and doped cases, respectively) show that the doping causes the band gap to be 19 meV smaller than that of the undoped one. If we neglect the effect of the

TABLE II. Charge transfer of NN Te and NNN cations for the doped case and average charge transfer in the atomic sphere for the undoped case. Subscripts "*crystal*" and "*atomic*" mean the crystal charge and the superposition of atomic charge, respectively. $\Delta Q = Q_{crystal} - Q_{atomic}$.

	$Hg_{0.5}Cd_{0.5}Te$-As_{Hg}			$Hg_{0.5}Cd_{0.5}Te$		
	$Q_{crystal}$	Q_{atomic}	ΔQ	$Q_{crystal}$	Q_{atomic}	ΔQ
As	31.699	31.469	0.23			
Te	49.958	49.730	0.228	49.947	49.730	0.217
Cd	46.628	46.541	0.087	46.576	46.541	0.035
Hg	78.466	78.398	0.068	78.424	78.398	0.026

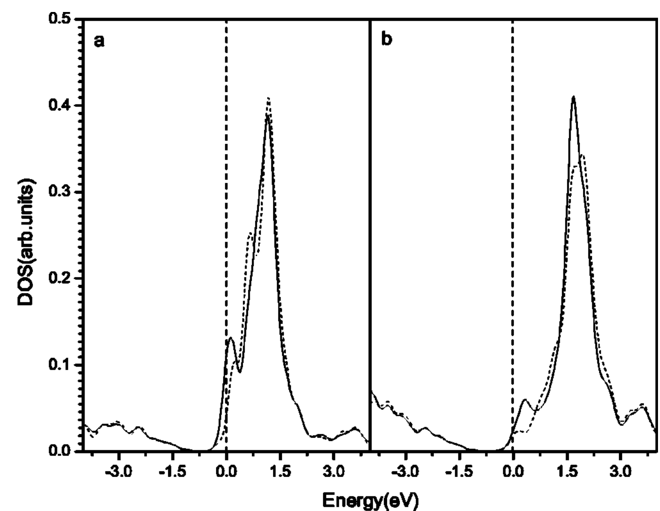

FIG. 5. The partial DOS of cation-s states with the different distance from the impurity. (a) and (b) are the Hg-s and Cd-s states, respectively. The solid and dashed lines are the NNN Hg (Cd) around the impurity and the Hg (Cd) furthest from the impurity in the supercell.

valence-band broadening on the band gap, the change can be ascribed to the donor state. The donor level can be qualitatively located in the region of less than 19 meV below the CBM. The quantitatively calculated results from the single-particle eigenvalues reveal that the donor level is 9 meV below the CBM, as a shallow donor. The results are in agreement with the experiment finding[27] for the As_{Hg}-doped MCT with stoichiometric $x=0.39$. It is well known that the calculation in terms of the LDA approximation cannot give the accurate band gap, as does the absolute position of the donor level for the present case. But the absolute energy positions calculated by the *ab initio* method are less significant than the relative ones.[28] In the meantime, the donor level has the *s*-like characteristics as mentioned above, so the relative position between the donor level and CBM, which is also derived from the *s* states of group II,[29] is accurate to some extent. Based on the relation between the ionization of the donor level and the mole fraction of MCT predicated by experiments,[30] we can predict that the As_{Hg} donor level will be shallower as the mole fraction becomes smaller. Especially, according to the most technologically important composition x around 0.2, the donor level is about 5 meV.

In summary, As_{Hg} doping on $Hg_{0.5}Cd_{0.5}Te$ produces some novel relaxations. The charge density and the DOS results reveal that the covalent bond between the impurity and the NN tellurium becomes stronger and the impurity induces a single donor level, quantitatively being 9 meV below the CBM, as a shallow donor. The coupling of the As impurity with the NN and NNN atoms at the band edge determines the optical transition of the doped materials.

This work is supported in part by the One-hundred-person Project of the Chinese Academy of Sciences (No. 200012), the Chinese National Key Basic Research Special Fund, the Key Fund of the Chinese National Science Foundation (No. 10234040), the Chinese National Science Foundation (No. 60221502 and No. 60476040), the Key Foundation of Shanghai Commision of Science and Technology (No. 02DJ14006), and the Shanghai Super-computer Center.

*Electronic address: xschen@mail.sitp.ac.cn

[1] G. F. Neumark, Mater. Sci. Eng., R. **21**, 1 (1997).
[2] M. A. Berding and A. Sher, Appl. Phys. Lett. **74**, 685 (1999).
[3] X. H. Shi, S. Rujirawat, R. Ashokan, C. H. Grein, and S. Sivananthan, Appl. Phys. Lett. **73**, 638 (1998).
[4] J. W. Garland, C. H. Grein, B. Yang, P. S. Wijewarnasuriya, F. Aqariden, and S. Sivananthan, Appl. Phys. Lett. **74**, 1975 (1999).
[5] H. R. Vydyanath, R. C. Abbott, and D. A. Nelson, J. Appl. Phys. **54**, 1323 (1983).
[6] H. R. Vydyanath, J. A. Ellsworth, and C. M. Devaney, J. Electron. Mater. **16**, 13 (1987).
[7] S. Sivananthan, P. S. Wijewarnauriya, F. Awariden, H. R. Vydyanath, M. Zandian, D. D. Edwall, and J. M. Arias, J. Electron. Mater. **26**, 621 (1997).
[8] X. H. Shi, S. Rujirawat, R. Ashokan, C. H. Grein, and S. Sivananthan, Appl. Phys. Lett. **73**, 638 (1998).
[9] T. C. Harman, J. Electron. Mater. **8**, 191 (1989).
[10] H. R. Vydyanath, Semicond. Sci. Technol. **5**, S213 (1990).
[11] M. A. Berding, A. Sher, M. Van Schilfgaarde, A. C. Chen, and J. Arias, J. Electron. Mater. **27**, 605 (1998).
[12] M. A. Berding and A. Sher, Appl. Phys. Lett. **74**, 685 (1999).
[13] M. Zandian, A. C. Chen, D. D. Edwall, J. G. Pasko, and J. M. Arias, Appl. Phys. Lett. **71**, 2815 (1997).
[14] P. S. Wijewarnasuriya, and S. Sivananthan, Appl. Phys. Lett. **72**, 1694 (1998).
[15] P. Hohenberg and W. Kohn, Phys. Rev. **136**, B864 (1964); W. Kohn and L. J. Sham, Phys. Rev. **140**, A1133 (1965).
[16] J. P. Perdew, K. Burke, and M. Ernzerhof, Phys. Rev. Lett. **77**, 3865 (1996).
[17] P. Blaha, K. Schwarz, G. Madsen, D. Kvasnicka, and J. Luitz, 2001WIEN2k, An Augmented Plane Wave + Local Orbitals Program for Calculating Crystal Properties (Karlheinz Schwarz, Techn. University Wien, Austria).
[18] Bernd Kohler, Steffen Wilke, and Matthias Scheffler, Comput. Phys. Commun. **94**, 31 (1996).
[19] R. Yu, D. Singh, and H. Krakauer, Phys. Rev. B **43**, 6411 (1991).
[20] B. Kohler *et al.*, Comput. Phys. Commun. **94**, 31 (1996).
[21] F. D. Murnaghan, Proc. Natl. Acad. Sci. U.S.A. **30**, 244 (1994).
[22] Sheng N. Sun, Nicholas Kioussis, Say-Peng Lim, A. Gonis, and William H. Gourdin, Phys. Rev. B **52**, 14 421 (1995).
[23] M. Iglesias, K. Schwarz, P. Blaha, D. Baldomir, Phys. Chem. Miner. **28**, 67 (2001).
[24] P. E. Blöchl, O. Jepsen, and O. K. Andersen, Phys. Rev. B **49**, 16 223 (1994).
[25] Su-huai Wei and S. B. Zhang, Phys. Rev. B **66**, 155211 (2002).
[26] Su-Huai Wei and Alex Zunger, Phys. Rev. B **43**, 1662 (1991).
[27] Y. Chang, J. H. Chu, W. G. Tang, W. z. Shen, and D. Y. Tang, Acta Phys. Sin. (Overseas Ed.) **4**, 66 (1995).
[28] Su-Huai Wei and Alex Zunger, Phys. Rev. B **37**, 8958 (1988).
[29] C. S. Wang and B. M. Klein, Phys. Rev. B **24**, 3393 (1981).
[30] A. T. Hunter and T. C. McGill, J. Appl. Phys. **52**, 5779 (1981); J. Vac. Sci. Technol. **21**, 205 (1982).